IET Renewable Power Generation

Research Article

IET Journals
The Institution of Engineering and Technology

Reactive power performance analysis of dish–Stirling solar thermal–diesel hybrid energy system

ISSN 1752-1416
Received on 14th June 2016
Revised 15th December 2016
Accepted on 1st February 2017
doi: 10.1049/iet-rpg.2016.0579
www.ietdl.org

Israfil Hussain[1] ✉, *Dulal Chandra Das*[1], *Nidul Sinha*[1]

[1]*Electrical Engineering Department, National Institute of Technology, Silchar, Assam 788010, India*

✉ *E-mail: israfilhussain1@gmail.com*

Abstract: Reactive power analysis of an autonomous hybrid energy system consisting of dish–Stirling solar thermal system (DSTS), diesel engine generator and static VAR compensator (SVC) has been conducted. Diesel engine coupled to a synchronous generator equipped with automatic voltage regulator (AVR) and DSTS is connected to an induction generator. The parameters of the proportional–integral controllers, employed with SVC and AVR are optimised simultaneously using genetic algorithm (GA), particle swarm optimisation (PSO) and flower pollination algorithm (FPA) techniques. The comparative performance of GA, PSO and FPA optimised controllers on the hybrid system model has been presented considering step change and random variations of solar thermal power as well as reactive power load. Simulation results revealed that FPA optimised controllers for AVR and SVC can provide the improved dynamic performance of the hybrid energy system as compared with GA and PSO optimised controllers.

Nomenclature

DSTS	dish–Stirling solar thermal system
AVR	automatic voltage regulator
SVC	static VAR compensator
SG	synchronous generator
IG	induction generator
P_{SG}, Q_{SG}	active and reactive powers generated by SG
Q_{SVC}	reactive power generated by SVC
Q_{Load}	reactive power load demand
Q_{IG}	reactive power required by IG
P_{IG}	mechanical input to the IG
P_{DSTS}	output power of the DSTS
P_{closs}	constant loss of the IG
V_{Rmax}, V_{Rmin}	maximum and minimum values of AVR output voltages
K_F	regulator stabilising circuit gain
T_F	regulator stabilising circuit time constant
T_A	regulator amplifier time constant
K_A	regulator gain p.u.
S_E	value of excitation function at E_{fdmax}
K_E	exciter constant for self-excited field
T_E	exciter time constant
$\Delta E'_q$	change in the internal armature emf of SG under transient condition
X_d	direct reactance of SG under transient condition
X_d	direct reactance of SG under steady-state condition
δ	load angle
ΔE_{fd}	p.u change in exciter voltage
ΔE_M	small change in the electromagnetic energy stored by IG
ΔB_{SVC}	small change in susceptance of the SVC
T_d	average dead time of zero crossing in a three-phase system
T'_{do}	direct axis open-circuit transient time constant
T_α	thyristor firing delay time
K_α	thyristor gain constant
α, $\alpha°$	thyristor firing angle and nominal thyristor firing angle
$\Delta\alpha$	small deviation in thyristor firing angle
ΔV, ΔV_{ref}, ΔV_a, ΔV_f	small change of terminal voltage, reference voltage, amplifier output voltage and exciter feedback voltage, respectively
R_{eq}, X_{eq}	equivalent resistance and equivalent reactance of the IG, respectively
Q_{SVC}	rating of SVC

1 Introduction

Dish–Striling solar thermal energy is a recent technology with its characteristics akin to wind energy and employs an asynchronous generator (squirrel-cage induction generator) [1, 2]. Dish–Stirling solar thermal system (DSTS) has the potential to provide a significant contribution to carbon free and sustainable energy generation and hence attracted research attention all over the world. The technology can be used as a stand-alone system or integration with other conventional technology [3, 4]. Nevertheless, power output from DSTS is fluctuating due to stochastic and unpredictable in nature of solar radiation [5]. Since DSTS is coupled with an induction generator reactive power absorbed by it also varies. Present work considers a DSTS-based autonomous hybrid energy system and investigates the reactive power control strategy. The topic has not been explored much. Other components of the hybrid energy system are diesel engine generator coupled with a synchronous generator (SG) and static VAR compensator (SVC). An induction generator (IG) which is connected to the grid can draw reactive power from the grid or can be supplied by the capacitor banks. However, in a stand-alone hybrid energy system as the proposed one, reactive power has to be supplied by the SG [6] as the fixed capacitors cannot meet the reactive power demand under varying solar thermal power and/or load conditions.

Moreover, any mismatch between reactive power demand and generation results in a deviation of system voltage from its nominal value [7]. The voltage deviations like over-voltage or under-voltage may affect the system performance in the form of insulation failure of equipments or system voltage collapse [8]. To mitigate this problem SVC has been proposed for the DSTS-based hybrid energy system.

Application of SVC and various types of SVC controllers in wind diesel-based hybrid power system have been reported in [7, 9–13]. In [7, 11, 12], voltage control issue of wind diesel-based power system using SVC, some very good works have been

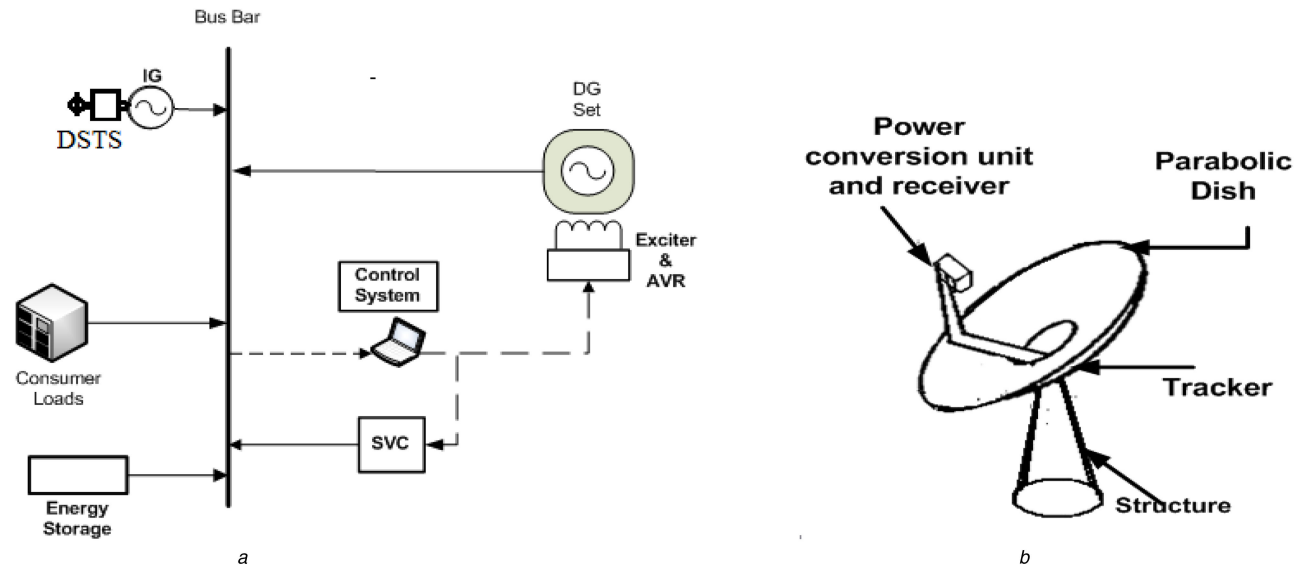

Fig. 1 *Proposed DSTS–DEG hybrid energy system*
(a) Schematic diagram of DSTS–DEG-based system, ***(b)*** Conceptual structure of DSTS

reported. However, the parameters of the SVC controllers were optimised keeping the parameters of automatic voltage regulator (AVR) control constant. This cannot ensure the proper coordination between the SVC and AVR controllers.

Vachirasricirikul *et al.* [13] presented voltage control of a wind diesel hybrid power system using H∞ loop shaping control of SVC and AVR with fixed-structure. In their work, the controller parameters of the SVC and AVR were optimised simultaneously by genetic algorithm (GA). The proposed voltage control method performed satisfactorily. The parameters of the SVC and AVR controllers were optimised under random load change with fixed reactive power consumption by the IG, which is not realistic. To include realistic features, the parameters should have been optimised simultaneously considering random variations of reactive power load as well as variations in the Q_{IG}.

The performance of the autonomous hybrid energy system also relies on the appropriate control mechanism and design of controllers. Ziegler–Nichols ultimate-cycle tuning, Cohen–Coon's, Astrom and Hagglund and so on are some of the common tuning methods of controller parameters. However, their applications are limited because of the complexities occurring during implementation [14]. Since power system is non-linear in nature, designing of controllers becomes difficult. Moreover, when the requirement is to optimise several gains of the controllers, conventional method for optimisation would be a difficult task [15]. Recently, automatic tuning of controller parameters using heuristics algorithms has gained much interest.

In view of the above, this work aims to investigate in detail the voltage control of a DSTS-based hybrid energy system with SVC. In which, the parameters of the PI (proportional plus integral) controllers employed with SVC and AVR are optimised simultaneously using GA, particle swarm optimisation (PSO) and flower pollination algorithm (FPA) techniques considering random variations of reactive power absorbed by the IG as well as the reactive load. This incorporates more realistic features in addition to improving its robustness against system disturbances and ensures the system stability. The contributions of this work are summarised as follows:

(i) Compared the performance of the DSTS-based hybrid system with and without SVC in containing the voltage fluctuations of the hybrid system model.
(ii) Optimise the parameters of PI controllers employed with SVC and AVR using GA, PSO and FPA techniques.
(iii) Compared the performance of FPA optimised PI controllers with their PSO and GA optimised counterparts on the hybrid system model for maintaining system voltage in the event of variations in any of the subcomponents, i.e. load, solar radiation or all.
(iv) Sensitivity analysis to study the robustness of PI controllers optimised at step disturbance conditions to significant changes in Q_{Load} and/ or Q_{IG}.
(v) Performance analysis of the hybrid system model for randomly varying conditions of reactive power load as well as reactive power absorbed by IG.

Remaining part of this paper is structured as follows: in Section 2, the mathematical modelling of hybrid system has been presented; Section 3 illustrates problem formulation. Simulation results and analysis have been presented in Section 4 and Section 5 covers the conclusions.

2 Mathematical modelling of components of the hybrid energy system

The proposed schematic diagram of hybrid energy system consists of DSTS (150 kW), diesel engine generator (DEG) (150 kW), load (250 kW), along with the conceptual structure of DSTS are shown in Figs. 1*a* and *b*, respectively. It may be noted that DEG is loaded 66.67% under normal operating condition. All constants and system data are taken from [13]. Power output from the DSTS, system voltage equation, and expressions of reactive power generated by SG, reactive power absorbed by IG, reactive power generated by SVC are discussed as follows.

2.1 Dish–Stirling solar thermal system

The constructional features and working of DSTS has been demonstrated in literatures [16–24]. The DSTS consists of the parabolic dish, receiver and the tracking device [24]. A receiver is located at the focus of the parabola. The parabolic dish concentrates the sunlight and focuses the same to the receiver [24]. The concentration ratio of the parabolic dish may go up to 3000 [23]. The receiver contains working fluid such as water, hydrogen or helium gas [19], which absorbs the heat energy. The thermal energy of the working fluid is converted to mechanical energy by the Stirling engine [17]. The Stirling engine, which acts as a prime mover, is coupled to a squirrel cage IG [18], and the induction generator generates electricity. The expression of output power as proposed in [17] is given by

$$P_{DSTS} = 0.015 P_m V_p f \tag{1}$$

where P_{DSTS}, P_m, f and V_p are the dish–Stirling solar thermal power output (watts), mean cycle pressure (bar), cycle frequency

(Hz) and displacement of power piston (cm^3), respectively. P_{DSTS} is fed to the IG as the input power (P_{IG}). Therefore, P_{DSTS} is equal to P_{IG}.

2.2 System voltage equation

In the proposed hybrid energy system, IG and reactive load are the reactive power absorbers, whereas SVC and SG are the sources. Therefore, considering steady-state condition [7], one can write

$$Q_{SG} + Q_{SVC} = Q_{Load} + Q_{IG} \tag{2}$$

Equation (2) gives the expression for reactive power generation and demand. Any kind of disturbance in Q_{Load} (i.e. ΔQ_{Load}) and/or Q_{IG} (i.e. ΔQ_{IG}) manifest into system voltage deviation (ΔV), which results in the SVC and SG to alter their reactive power generation by ΔQ_{SVC} and ΔQ_{SG}, respectively. In this situation, any excess reactive power in the system can be calculated as $\Delta Q_{SG} + \Delta Q_{SVC} - \Delta Q_{Load} - \Delta Q_{IG}$ [7, 11–13]. This excess power will improve the system voltage [7] which in Laplace form [7, 11–13, 25–29], is given by

$$\Delta V(s) = \frac{K_V}{1 + sT_V}[\Delta Q_{SG}(s) + \Delta Q_{SVC}(s) - \Delta Q_{Load}(s) - \Delta Q_{IG}(s)] \tag{3}$$

where $T_V = 2H_r/D_V V^o$ and $K_V = 1/D_V$ are the system time constant and gain, respectively, and $D_V = (\partial Q_{Load}/\partial V)$.

2.3 Synchronous generator

The SG of the proposed hybrid energy system employs an IEEE type-1 excitation control system as described in [26]. The expressions for ΔE_{fd}, ΔV_a and ΔV_f in Laplace form [25, 28, 29] can be written as

$$\Delta E_{fd}(s) = \frac{1}{K_E + sT_E}\Delta V_a(s) \tag{4}$$

$$\Delta V_a(s) = \frac{K_A}{1 + sT_A}\left[-\Delta V(s) - \frac{K_F}{T_F}\Delta E_{fd}(s) + \Delta V_{ref}(s)\right] \tag{5}$$

$$\Delta V_f(s) = \frac{K_F/T_F}{1 + sT_F}\Delta E_{fd}(s) \tag{6}$$

Under small disturbance conditions, the internal armature voltage [28] of the SG changes. The expression which describes the change in $\Delta E'_q$ has been derived in [29], in Laplace transform it becomes

$$\Delta E'_q(s) = \frac{1}{(1 + sT_G)}K_1\Delta E_{fd}(s) + K_2\Delta V(s) \tag{7}$$

In (7), K_1 and K_2 [28] are given as

$$K_1 = \frac{x'_d}{x_d} \text{ and } K_2 = \{(x_d - x'_d)\cos\delta\}/x_d \tag{8}$$

$$T_G = T'_{do}\frac{x'_d}{x_d} \tag{9}$$

Considering small disturbance, the expression for reactive power generated by the Q_{SG} is given by [28, 29]

$$Q_{SG} = \frac{E'_q V\cos\delta - V^2}{x'_d} \tag{10}$$

For incremental change (10) can be expressed [27] by

$$\Delta Q_{SG} = \frac{V\cos\delta}{x'_d}\Delta E'_q + \frac{E'_q\cos\delta - 2V}{x'_d}\Delta V \tag{11}$$

Equation (11) in Laplace transform [5, 9–11, 27] becomes

$$\Delta Q_{SG}(s) = K_3\Delta E'_q(s) + K_4\Delta V(s) \tag{12}$$

where

$$K_3 = \frac{V\cos\delta}{x'_d} \text{ and } K_4 = \frac{E'_q\cos\delta - 2V}{x'_d} \tag{13}$$

2.4 Induction generator

For the detailed mathematical modelling of IG authors may refer to [29]. For constant slip operation, the incremental Q_{IG} is given by

$$\Delta Q_{IG}(s) = \frac{2VX_{eq}}{R_Y^2 + X_{eq}^2}\Delta V(s) \tag{14}$$

$$\Delta Q_{IG}(s) = K_5\Delta V(s) \tag{15}$$

where

$$K_5 = \frac{2VX_{eq}}{R_Y^2 + X_{eq}^2} \tag{16}$$

Now, considering a variable slip IG, the expression for incremental reactive power is given by [29]

$$\Delta Q_{IG}(s) = K_{5'}\Delta P_{IG}(s) + K_{5''}V(s) \tag{17}$$

where

$$K_{5'} = \frac{Q_{IG}}{P_{IG} - P_{closs} - (1/2)(V^2/R_Y)} \tag{18}$$

$$K_{5''} = \frac{2V}{R_Y^2 + X_{eq}^2}\left[X_{eq} - \frac{R_P Q_{IG}}{P_{IG} - P_{closs} - (1/2)(V^2/R_Y)}\right] \tag{19}$$

R_Y and X_{eq} are given in detail in [27]. In (17)–(19), P_{IG} is equal to P_{DSTS}.

2.5 Static Var compensator

In the proposed hybrid energy system, SVC reduces the difference between the generation of reactive power and its demand. The FC-TCR type configuration of SVC controller [7, 11–13, 29], has been considered for this work. The equivalent fixed capacitor-thyristor controlled reactor (FC-TCR) circuit and the SVC model are shown in Figs. 2*a* and *b*, respectively. For detailed mathematical modelling of SVC readers may refer to [29].

Q_{SVC} supplied by the SVC is given by [7, 11–13, 29]

$$Q_{SVC} = B_{SVC}V^2 \tag{20}$$

For small disturbance, (20) can be written as [7, 11–13, 29]

$$\Delta Q_{SVC} = 2VB_{SVC}\Delta V + V^2\Delta B_{SVC} \tag{21}$$

$$= K_6\Delta V + K_7\Delta B_{SVC} \tag{22}$$

where

$$K_6 = 2VB_{SVC} \text{ and } K_7 = V^2 \tag{23}$$

The expressions for ΔV_{SVC}, $\Delta B'_{SVC}$, $\Delta\alpha$ can be written as [7, 11–13, 29]

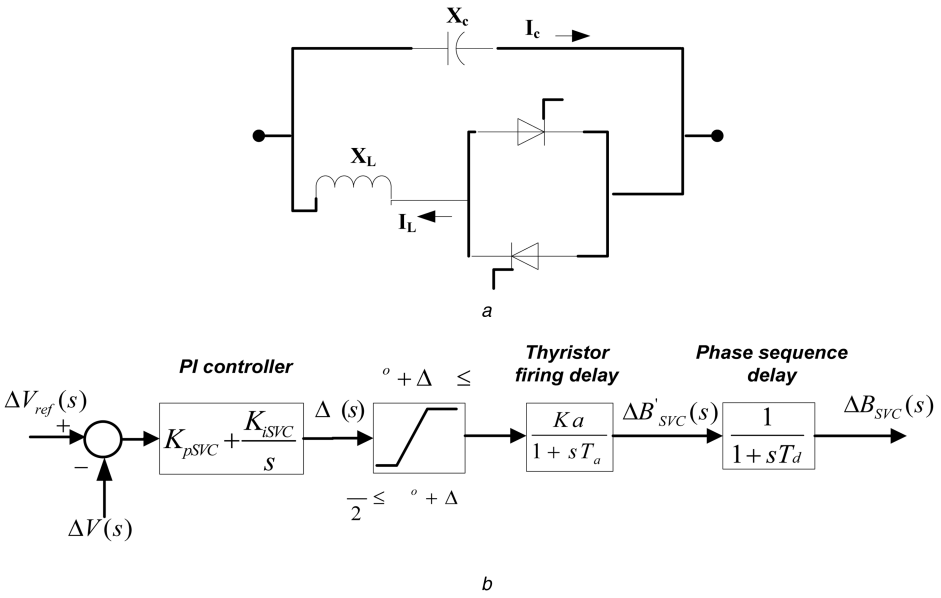

Fig. 2 *SVC system*
(a) Equivalent FC-TCR circuit of SVC, ***(b)*** SVC model [11]

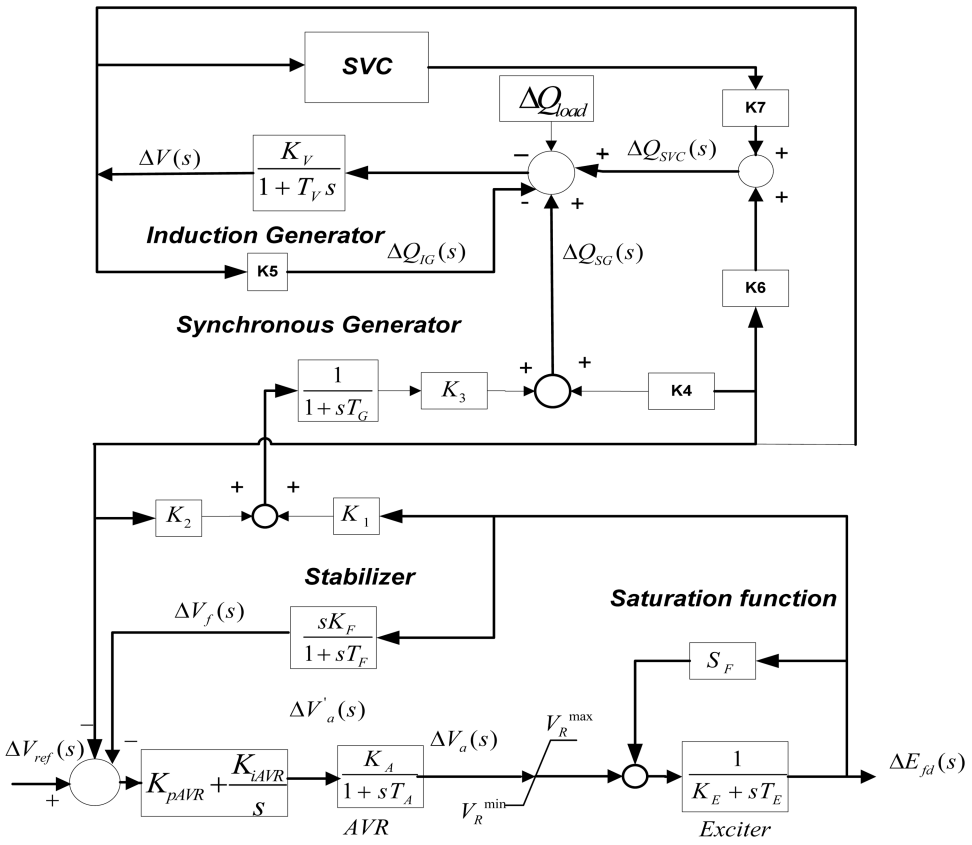

Fig. 3 *Transfer function block diagram of DSTS–DEG hybrid energy system*

$$\Delta V_{\mathrm{SVC}}(s) = \frac{1}{1+sT_d}\Delta B'_{\mathrm{SVC}}(s) \tag{24}$$

$$\Delta B'_{\mathrm{SVC}}(s) = \frac{K_\alpha}{1+sT_\alpha}\alpha(s) \tag{25}$$

$$\Delta\alpha(s) = \left(K_{\mathrm{pSVC}} + \frac{K_{\mathrm{iSVC}}}{s}\right)\left(\Delta V_{\mathrm{ref}}(s) - \Delta V(s)\right) \tag{26}$$

Combining all the expressions a transfer function model has been developed, as shown in Fig. 3.

3 Problem formulation

To provide the coordinated control between the SVC and AVR, the gains of the PI controllers are optimised simultaneously considering different operating conditions. The objective function is the integrated absolute error (IAE) of voltage deviation, which is given by

$$J = \int_0^T (|\Delta v|)\,\mathrm{d}t \tag{27}$$

where T is the simulation time and Δv is the voltage deviation. The main objective is to optimise the controllers parameters, i.e. to

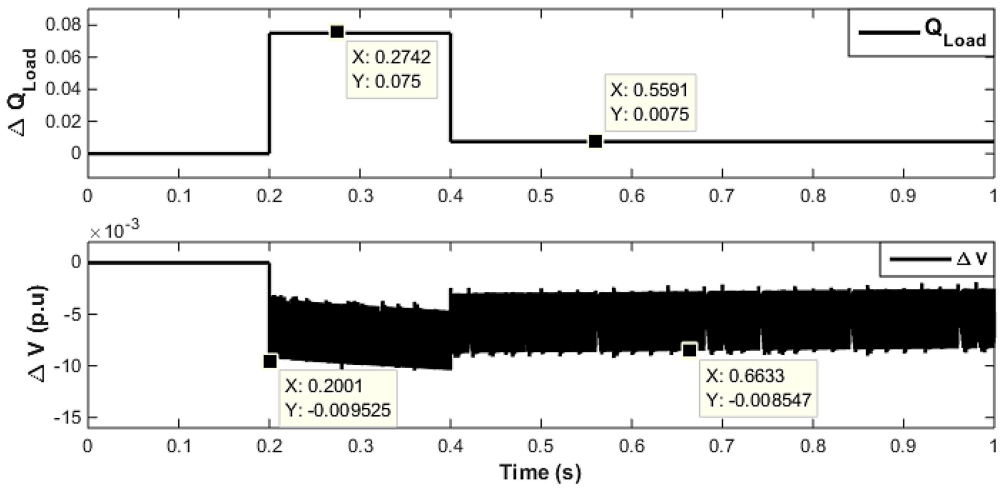

Fig. 4 *ΔQ_{Load} and ΔV of the hybrid system without SVC under step disturbances in Q_{Load}, case 1*

minimise the performance index J by optimising the controllers gains. Therefore, main objective is to

$$\text{Minimise } J$$

Subject to

$$K_{\text{pSVC}}^{\min} \le K_{\text{pSVC}} \le K_{\text{pSVC}}^{\max} \tag{28}$$

$$K_{\text{iSVC}}^{\min} \le K_{\text{iSVC}} \le K_{\text{iSVC}}^{\max} \tag{29}$$

$$K_{\text{pAVR}}^{\min} \le K_{\text{pAVR}} \le K_{\text{pAVR}}^{\max} \tag{30}$$

$$K_{\text{iAVR}}^{\min} \le K_{\text{iAVR}} \le K_{\text{iAVR}}^{\max} \tag{31}$$

where K_{p} and K_{i} are the proportional and integral gains, respectively. The objective function is minimised by optimising the controller parameters as shown in (28)–(31) using GA, PSO and FPA.

Controller parameters are optimised using GA, PSO and FPA techniques. These techniques are being applied in solving several types of optimisation problems, e.g. highly non-linear, highly complex, discontinuous, non-differentiable problems [30]. For the detailed study and the steps followed in optimising controllers' gains using these techniques readers may refer to [31–37]. The ranges of K_{p}, and K_{i} for SVC and AVR are presented in Table 1 and the tuned parameters of GA, PSO and FPA techniques are presented in Table 2.

4 Results and analysis

Table 1 Ranges of the variables

Variables	Minimum	Maximum
K_{p}	10	600
K_{i}	1	25,000

Time-domain simulated responses of the proposed hybrid energy system under various operating and disturbance conditions are analysed in this section.

4.1 Dynamic performance analysis of the hybrid system without SVC under step load disturbances: case 1

The nominal value of reactive power absorbed by the Q_{Load} is 0.75 p.u under normal operating conditions. To investigate the transient performance of the autonomous hybrid energy system without SVC, step changes in Q_{Load} are considered. At $t = 0.2$ s Q_{Load} rises by 10% of its nominal value of 0.75 p.u. (i.e. $\Delta Q_{\text{Load}} = 0.075$) and it reduces to 0.0075 p.u (i.e. 1% of nominal value) at $t = 0.4$ s. In this case study, P_{IG} (=P_{DSTS}) is constant (i.e. IG operating at constant slip). Fig. 4 shows the step changes in Q_{Load} and corresponding voltage deviations. It has been found that with the step load perturbations, there are considerable voltage variations and the automatic voltage regulator employed with SG is not capable of maintaining the system voltage at the required level. Thus, the system demands for a reactive power compensation device to mitigate mismatch in the reactive power, and thereby stabilise the responses.

4.2 Dynamic performance analysis of the hybrid energy system with SVC under step change in reactive power load: case 2

The transient response of the system with SVC under step disturbances in reactive power (ΔQ_{Load}) has been investigated and analysed in this case study. Fig. 5*a* presents the step changes in reactive power (ΔQ_{Load}) absorbed by the load. At $t = 0.2$ s, Q_{Load} rises by 10% of its nominal value of 0.75 p.u. (i.e. ΔQ_{Load} 0.075) and it reduces to 0.0075 p.u (i.e.1% of nominal value) at $t = 0.4$ s. It may be noted that in this case study, P_{IG} (=P_{DSTS}) is constant (i.e. IG operating at constant slip). Fig. 5*b* presents transient response for voltage deviation of the hybrid energy system. It can be observed that when there is a rise in reactive power demand at $t =$ 0.2 s, generator terminal voltage decreases showing a sharp deviation. Again, at $t = 0.4$ s, as the reactive power demand decreases, the terminal voltage rises resulting a deviation. Due to

Table 2 Parameters of GA, PSO and FPA

GA parameters	Value	PSO parameters	Value	FPA parameters	Value
maximum number of generations	100	maximum number of iterations	100	maximum number of generations	100
population size	50	population size	50	population size	50
crossover probability	0.8	$\omega_{\max}$	0.9	switch probability	0.8
mutation probability	0.01	$\omega_{\min}$	0.1		
		C_1	2		
		C_2	2		

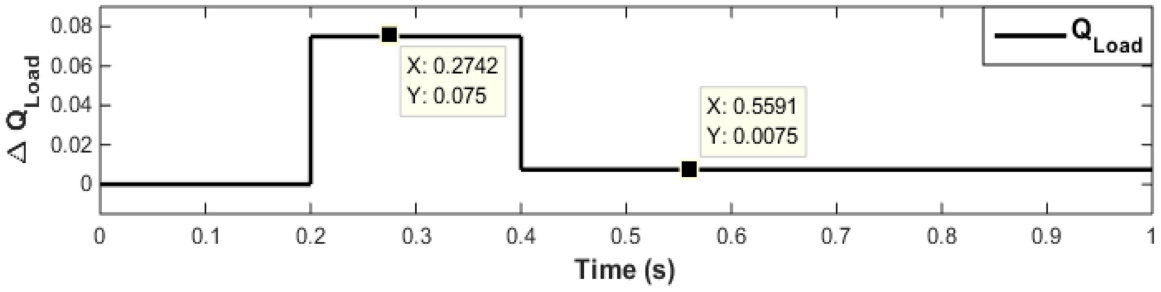

a

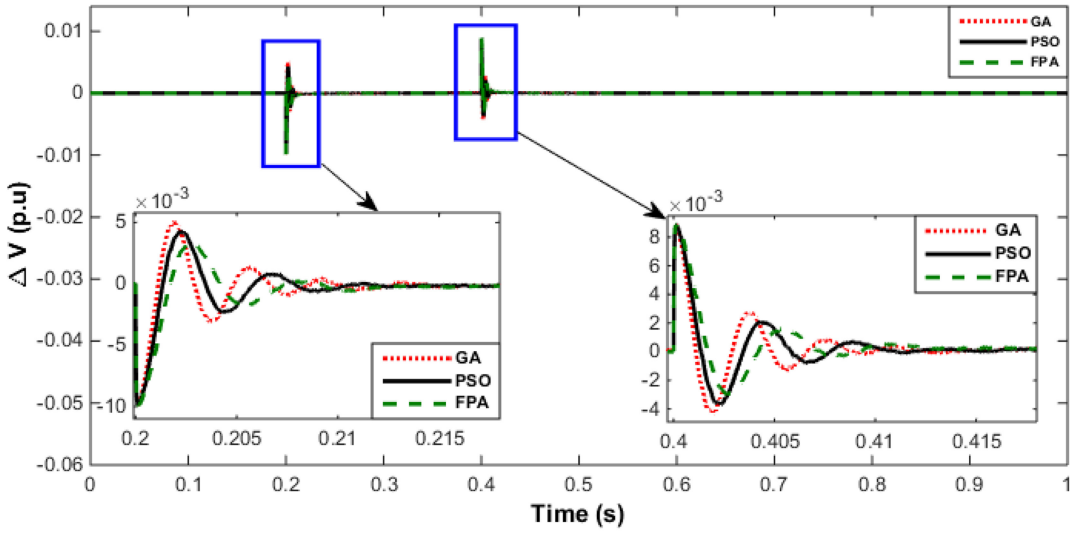

b

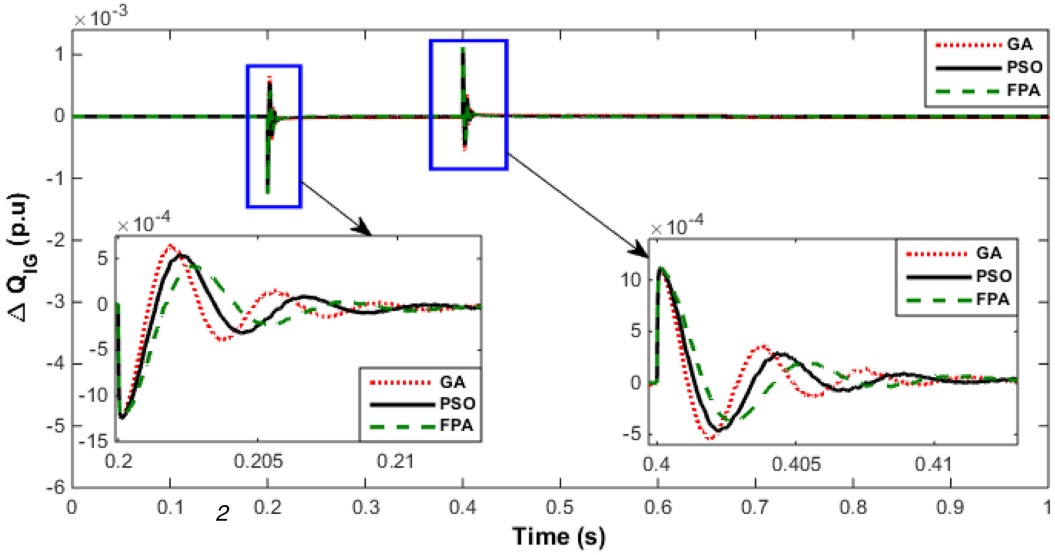

c

the action of the SVC and AVR controllers, the voltage deviations in both the cases decay very quickly.

The transient responses of ΔQ_{IG}, ΔQ_{SVC} and ΔQ_{SG} for the hybrid system with SVC are presented in Figs. 5*c*–*e*, respectively. Although P_{DSTS} is constant, due to mismatch in reactive power as a result of step disturbance in reactive power demand at $t = 0.2$ s and 0.4 s, the reactive power absorbed by the IG also is disturbed momentarily (Fig. 5*c*). Fig. 6 depicts the convergence plots of objective function values versus generation/iteration for GA, PSO and FPA optimised PI controllers. It is seen that the objective function curve obtained with FPA algorithm converges faster than the other two.

4.3 Dynamic performance analysis of the hybrid system with SVC, under step changes in Q_{Load} as well as P_{DSTS}: case 3

This section investigates the transient responses of the hybrid energy system for step changes in Q_{Load} as well as P_{DSTS}. Fig. 7*a* presents the step changes in reactive power (ΔQ_{Load}), and the step change in P_{DSTS}. As because $P_{IG} = P_{DSTS}$, any variation in the P_{DSTS} implies change in input power to the IG (P_{IG}), which in turn reflects in the slip of the IG. Reactive power absorbed by the IG is a function of mechanical input to the IG (P_{IG}), as in (17)–(19). At $t = 0.2$ s Q_{Load} rises by 10% of its nominal value of 0.75 p.u. (i.e. ΔQ_{Load} 0.075) and it reduces to 0.0075 p.u. (i.e. 1% of nominal value) at $t = 0.4$ s. Whereas, at $t = 0$ s, P_{DSTS} rises to 0.08 p.u., further, at $t = 0.6$ s, it rises to 0.1 p.u and at $t = 0.8$ s it gets reduced to 0.05 p.u. Fig. 7*b* presents the transient response for voltage

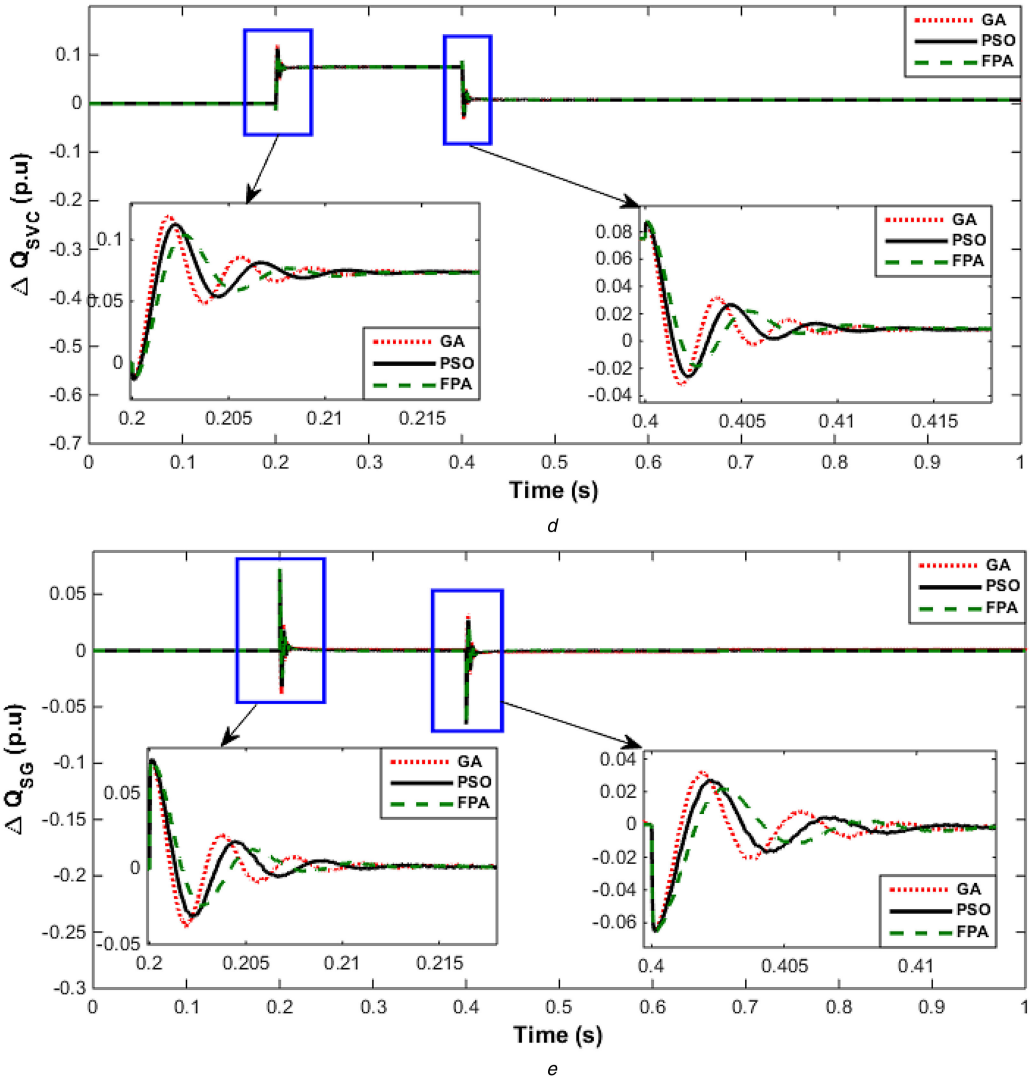

Fig. 5 *Dynamic responses of the hybrid energy system when employed with SVC, under step load changes Q_{Load} case 2*

(a) Step disturbances in Q_{Load}, ***(b)*** Dynamic responses of ΔV, ***(c)*** Dynamic responses of ΔQ_{IG}, ***(d)*** Dynamic responses of ΔQ_{SVC}, ***(e)*** Dynamic responses of ΔQ_{SG}

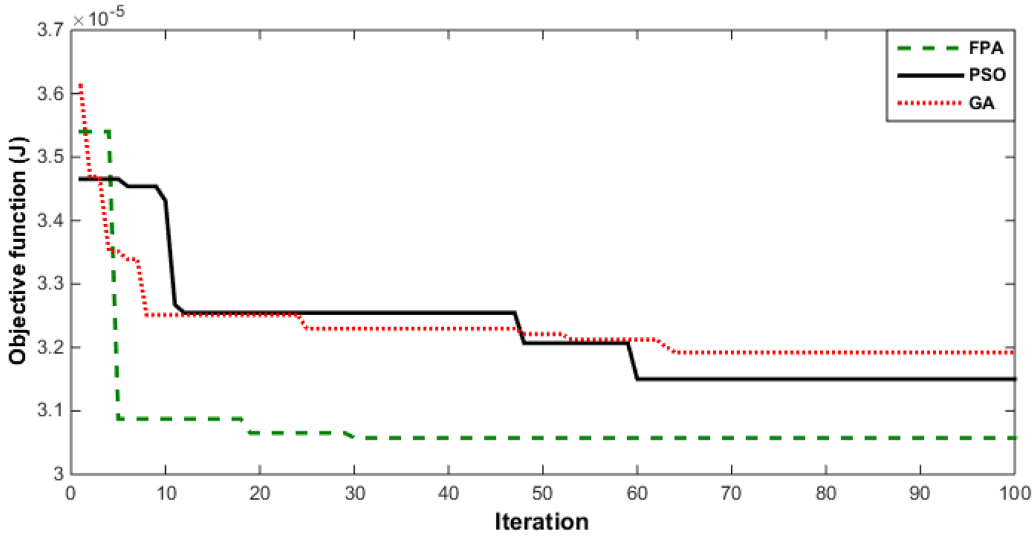

Fig. 6 *Convergence plots of objective function value versus generation/iteration for the model with GA, PSO and FPA optimised PI controller, case 2*

deviation of the hybrid energy system. It may be noted that when there is a rise in reactive power demand at $t = 0.2$ s, generator terminal voltage decreases showing a sharp deviation. Again, at $t = 0.4$ s, as the reactive power demand decreases the terminal voltage rises resulting a deviation. Due to the action of the SVC and AVR controllers, the voltage deviations in both the cases are settled down to zero very quickly. The transient responses of ΔQ_{IG}, ΔQ_{SVC} and ΔQ_{SG} for the hybrid system with SVC are presented in Figs. 7*c–e*, respectively. It is evident from the results presented in this section that FPA optimised controllers are superior to their GA and PSO optimised counterparts.

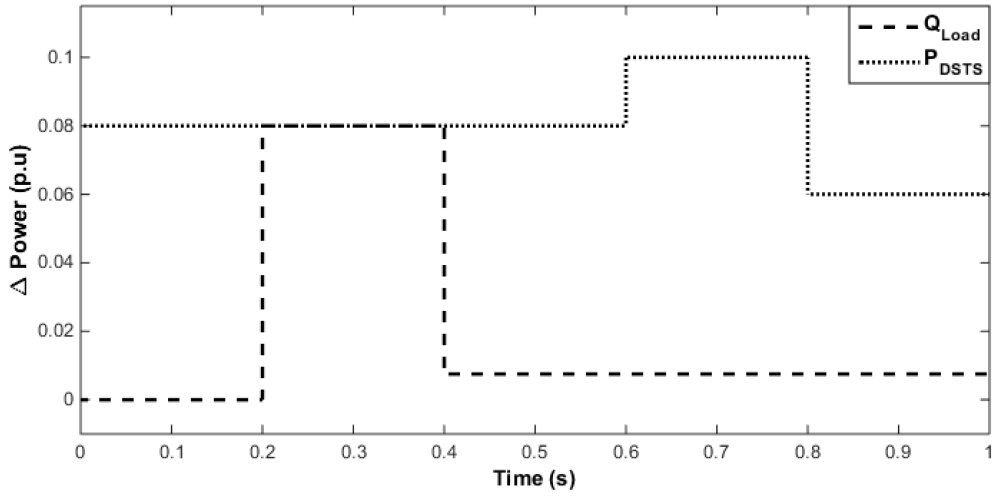

a

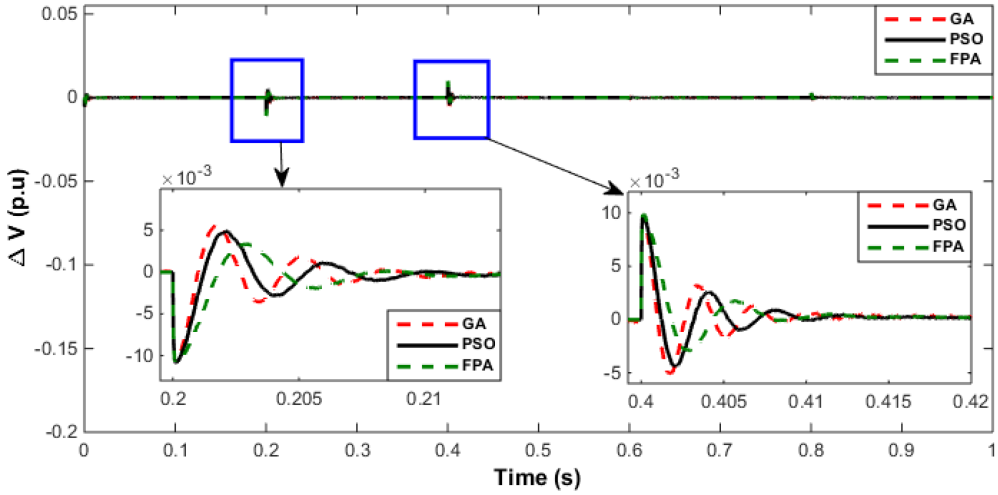

b

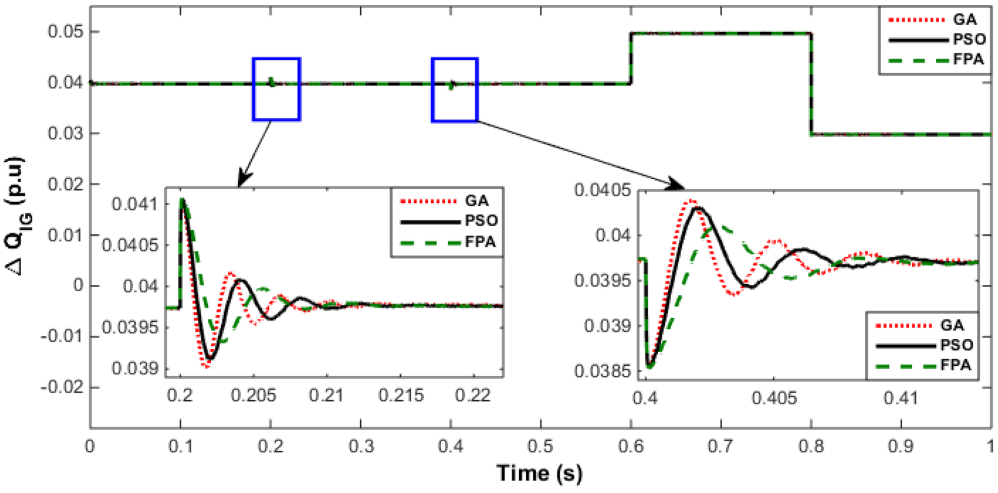

c

Further, this section examines the robustness of gains of the SVC and AVR controller parameters against the system uncertainties by carrying out sensitivity analysis. The controllers with their gains as obtained in case 2, are employed in case 3 and their comparative performance vis-à-vis their counterparts obtained at step changes in Q_{Load} as well as P_{DSTS} (case 3) has been presented. Results of ΔV under this situation are depicted in Fig. 7*f*.

The responses revealed that the FPA optimised gains of PI controllers obtained in case 2 (i.e. at constant slip) work well under significant changes in the system loading or changes in slip of the IG.

4.4 Dynamic performance analysis of the hybrid system with SVC under random variations of Q_{Load} and Q_{IG}, i.e. output power of DSTS: case 4

To assess the effects of variable nature of Q_{Load} and Q_{IG} on the performance of the hybrid system, their random variations have been considered while optimising the controller parameters. Reactive power absorbed by the IG is a function of mechanical input to the IG (P_{IG}), as in (17)–(19). Further, mechanical input power to IG is the output power of DSTS (P_{DSTS}), which is given in (1). Randomly variable output power P_{DSTS} has been considered

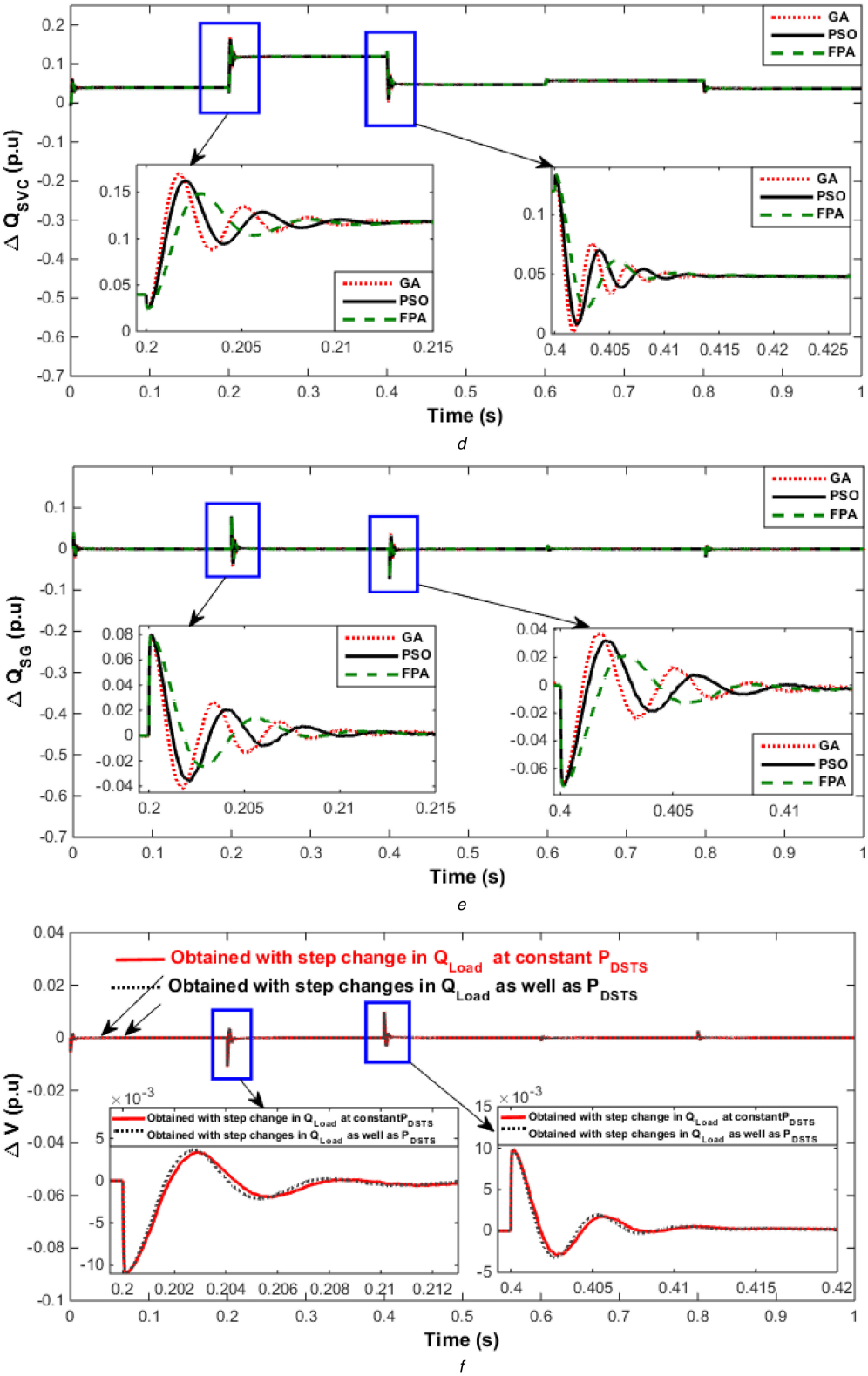

Fig. 7 *Dynamic responses of the hybrid energy system when employed with SVC, under step load changes Q_{Load} and P_{DSTS}, case 3*

(a) Step change in reactive power load Q_{Load} and P_{DSTS}, ***(b)*** Dynamic responses of ΔV, ***(c)*** Dynamic responses of ΔQ_{IG}, ***(d)*** Dynamic responses of ΔQ_{SVC}, ***(e)*** Dynamic responses of ΔQ_{SG}, ***(f)*** Sensitivity analysis of FPA optimised PI controller, in terms of voltage deviations

in this study. Fig. 8*a* presents the P_{DSTS} and Q_{Laod} under randomly varying conditions, which are applied in this study.

The random variations in the Q_{Load} and Q_{IG}, result in voltage fluctuations at the generator terminal. Due to the action of the SVC and AVR controllers, the reactive power generated by the SG as well as SVC varies accordingly so as to mitigate the difference between the total reactive power demand and total reactive power generation (i.e. to make $\Delta Q_{\text{SG}} + \Delta Q_{\text{SVC}} - \Delta Q_{\text{IG}} - \Delta Q_{\text{Load}} = 0$). This in turn eliminates the voltage deviations. The results of ΔV, ΔQ_{IG}, ΔQ_{SVC} and ΔQ_{SG} and under this situation, are depicted in Figs. 8*b*–*e*, respectively.

Further, this section examines the robustness of gains of the SVC and AVR controller parameters against the system uncertainties by carrying out sensitivity analysis. The controllers with their gains as obtained in case 2, are employed in case 4 and their comparative performance vis-à-vis their counterparts obtained at randomly varying Q_{Load} and Q_{IG} (case 4) has been presented. Results of ΔV under this situation are depicted in Fig. 8*f*. The

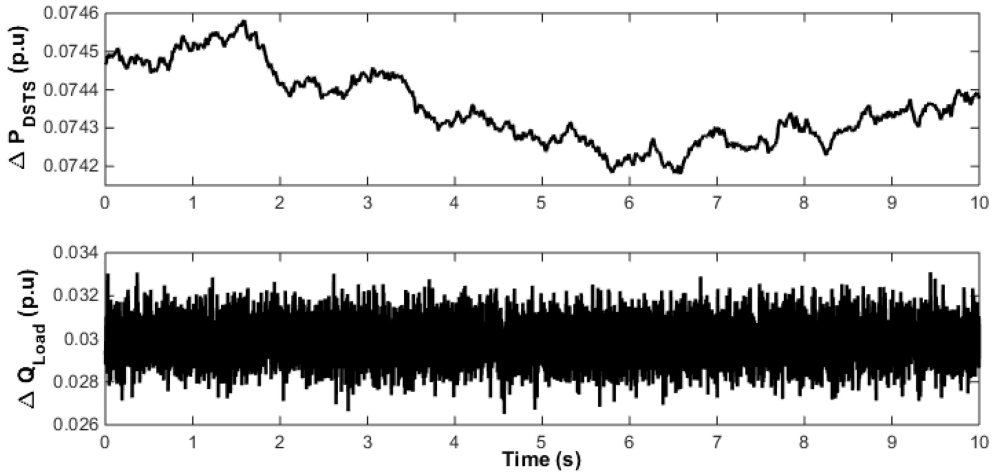

a

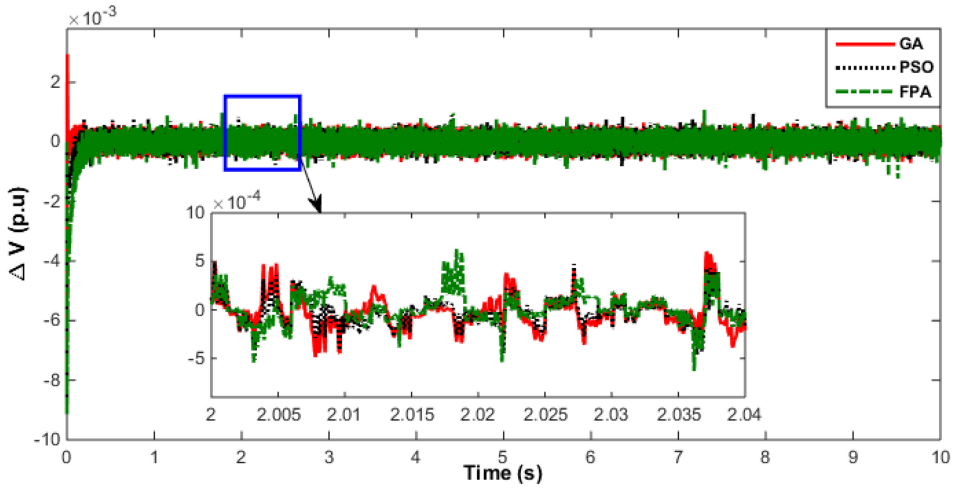

b

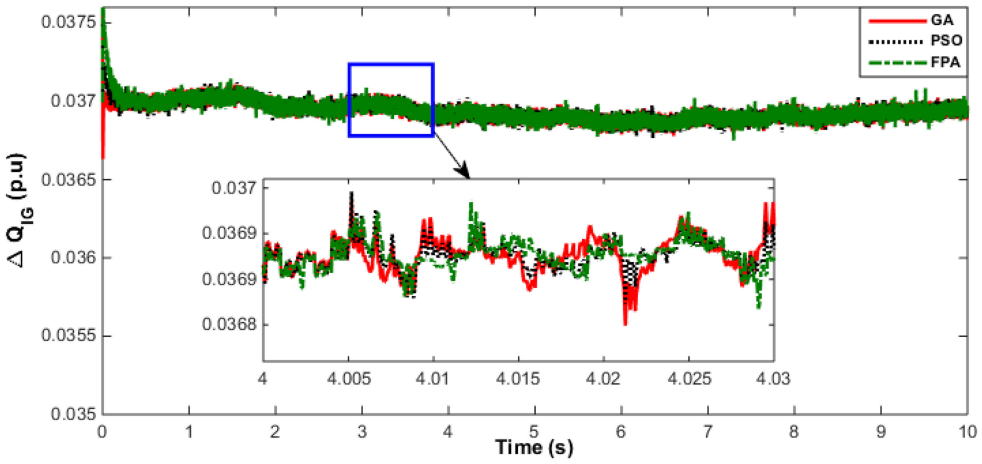

c

dynamic responses indicated that the optimum parameters of PI controllers obtained in case 2 (i.e. at constant slip), work well under uncertainties like significant changes in the system loading or variable slip of IG.

The values of PI controllers' parameters optimised using GA, PSO and FPA at randomly varying Q_{Load} and Q_{IG} are presented in Tables 3–5, respectively. Table 6 presents the maximum voltage deviations (ΔV) for the model using GA, PSO and FPA optimised controllers during small perturbations.

5 Conclusions

Voltage control strategy of DSTS-based autonomous hybrid energy system is thoroughly investigated for the first time. The SVC, in addition to SG, provides variable reactive power to meet the reactive power demand by the load and/ or IG employed with DSTS system under varying conditions. A complete dynamic hybrid system model has been developed to investigate the effect of load disturbances and/ or change in P_{DSTS}. To ensure the coordinated control, the parameters of SVC and AVR controllers' are optimised simultaneously considering uncertainties as mentioned in the case studies. GA, PSO and FPA are applied in optimising the controller parameters. The significant contributions from this work are as follows:

i. The transient performance of the dish–Stirling-based hybrid system without SVC has been conducted at step changes in Q_{Load}. Result indicated that the voltage deviations are considerably large, AVR employed with SG is not capable of maintaining the system voltage at the required level. To

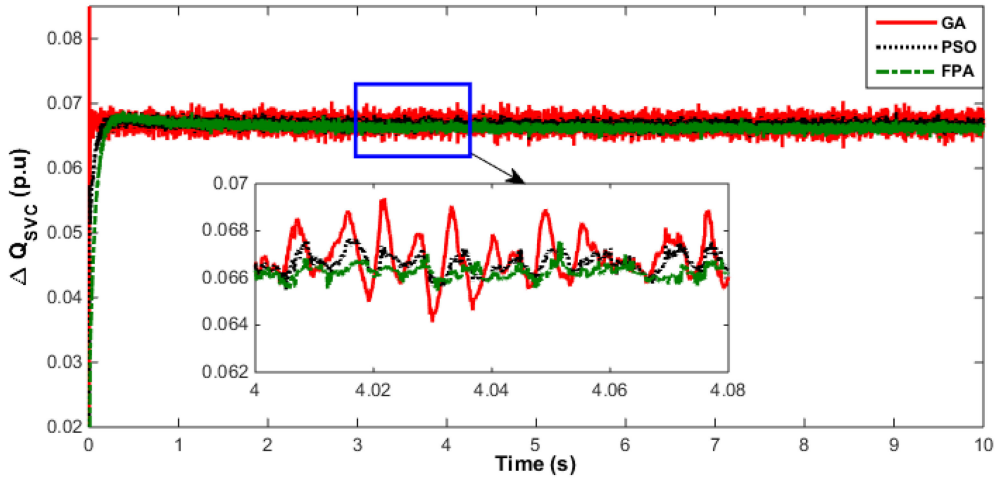

d

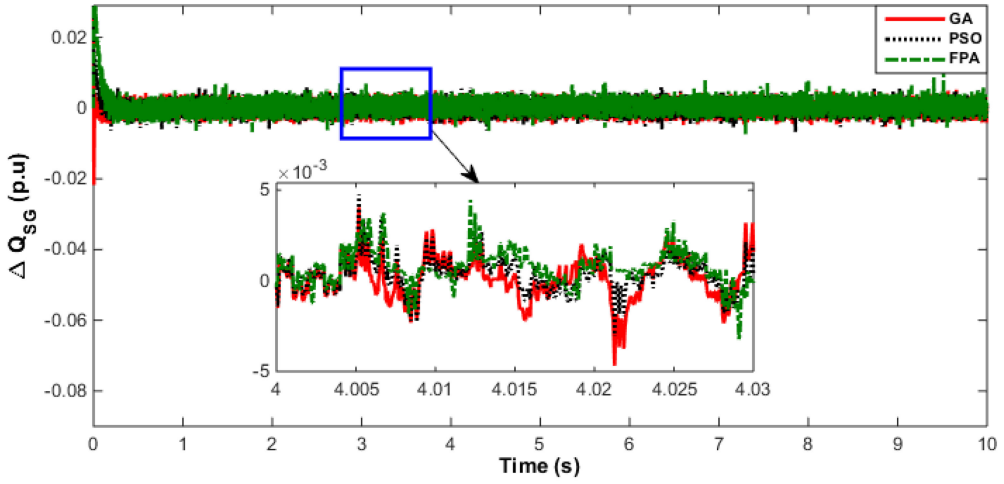

e

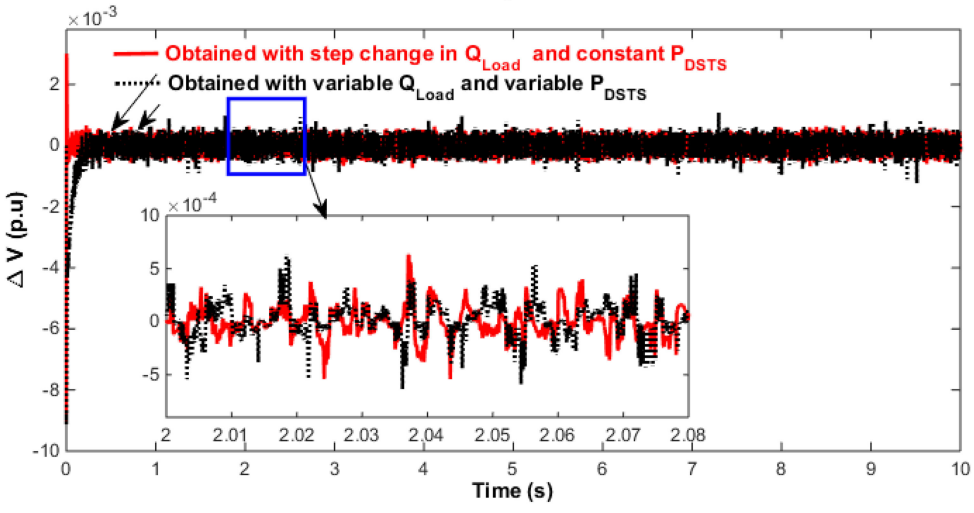

f

Fig. 8 *Dynamic responses of the hybrid energy system when employed with SVC, under random variations in Q_{Load} and P_{DSTS} case 4*

(a) Random variations Q_{Load} and P_{DSTS}, ***(b)*** Dynamic responses of ΔV, ***(c)*** Dynamic responses of ΔQ_{IG}, ***(d)*** Dynamic responses of ΔQ_{SVC}, ***(e)*** Dynamic responses of ΔQ_{SG}, ***(f)*** Sensitivity analysis of FPA optimised PI controller for case 4, in terms of voltage deviations

Table 3 Values of the GA optimised PI controllers' parameters

Gains	Case 2	Case 3	Case 4
K_{pSVC}	406	473	163
K_{iSVC}	21,891	19,868	15,461
K_{pAVR}	49	66.087	87
K_{iAVR}	125	1.2087	111

mitigate the voltage deviation, the system needs a reactive power compensation device such as SVC.

ii. The dynamic responses show that coordinated control of SVC and AVR with their gains tuned by GA, PSO and FPA techniques can provide improved dynamic performance of the hybrid energy system in containing voltage deviation.

iii. Comparative performance of FPA optimised PI controller with GA and PSO optimised PI controllers indicated that the response of FPA optimised PI controller is better than its GA

Table 4 Values of the PSO optimised PI controllers' parameters

Gains	Case 2	Case 3	Case 4
K_{pSVC}	289	333.114	50.1157
K_{iSVC}	18,667	17,889	1175.9
K_{pAVR}	175	121.65	104.1065
K_{iAVR}	125	25.2612	64.3865

Table 5 Values of the FPA optimised PI controllers' parameters

Gains	Case 2	Case 3	Case 4
K_{pSVC}	200.13	175.24	15.47
K_{iSVC}	12,010	11001.40	445.53
K_{pAVR}	79.02	214.31	140.12
K_{iAVR}	221.98	45.87	40

Table 6 Maximum voltage deviations (ΔV) in p.u. for the model using GA, PSO and FPA optimised controller during small perturbations

Cases	Techniques	$t = 0.2$ s	$t = 0.4$ s
case 2	GA	0.005219	−0.004340
	PSO	0.004178	−0.003442
	FPA	**0.00329**	**−0.002911**
case 3	GA	0.005732	−0.005005
	PSO	0.004442	−0.004266
	FPA	**0.003329**	**−0.002712**

and PSO optimised counterpart in terms of peak transient deviation and settling time.

iv. Compared the performance of FPA optimised PI controllers optimised with step change and their counterparts optimised under randomly varying conditions, revealed that the optimum gain values optimised with step change conditions are quite robust and work well under uncertainties like significant changes in the system loading conditions and or variable reactive power absorbed by the IG.

v. Finally, it can be concluded from the simulation results that FPA-based optimisation technique is much better to tune automatic voltage control of a DSTS-based autonomous hybrid system.

6 Acknowledgment

The authors thank Electrical Engineering Department, NIT Silchar, for providing the necessary facilities for completing this work.

7 References

[1] Howard, D.F., Liang, J., Harley, R.G.: 'Control of receiver temperature and shaft speed in dish-Stirling solar power'. IEEE Energy Conversion Congress and Exposition (ECCE), 2010, pp. 398–405

[2] Howard, D.F., Harley, R.G.: 'Modeling of dish-Stirling solar thermal power generation'. IEEE PES, General Meeting, 2010, pp. 1–7

[3] Aichmayer, L., Spelling, J., Laumert, B., *et al.*: 'Micro gas-turbine design for small-scale hybrid solar power plants', *J. Eng. Gas Turbines Power*, 2013, **135**, (11), p. 113001

[4] Bravo, Y., Monné, C., Bernal, N., *et al.*: 'Hybridization of solar dish-Stirling technology: analysis and design', *Environ. Prog. Sustain. Energy*, 2014, **33**, (4), pp. 1459–1466

[5] Li, Y., Choi, S.S., Yang, C., *et al.*: 'Design of variable-speed dish-Stirling solar–thermal power plant for maximum energy harness', *IEEE Trans. Energy Convers.*, 2015, **30**, (1), pp. 394–403

[6] Bansal, R.C.: 'Three-phase self-excited induction generators (SEIG): an overview', *IEEE Trans. Energy Convers.*, 2005, **20**, (2), pp. 292–299

[7] Bansal, R.C.: 'Automatic reactive-power control of isolated wind diesel hybrid power systems', *IEEE Trans. Ind. Electron.*, 2006, **53**, (4), pp. 1116–1126

[8] Del Valle, Y., Venayagamoorthy, G.K., Mohagheghi, S., *et al.*: 'Particle swarm optimization: basic concepts, variants and applications in power systems', *IEEE Trans. Evol. Comput.*, 2008, **12**, (2), pp. 171–194

[9] Cheng, C.H., Hsu, Y.Y.: 'Damping of generator oscillations using an adaptive static var compensator', *IEEE Trans. Power Syst.*, 1992, **7**, (2), pp. 718–725

[10] Al-Alawi, S.M., Ellithy, K.A.: 'Tuning of SVC damping controllers over a wide range of load models using an artificial neural network', *Int. J. Electr. Power Energy Syst.*, 2000, **22**, (6), pp. 405–420

[11] Bansal, R.C.: 'ANN based reactive power control of isolated wind diesel micro-hydro hybrid power systems', *Int. J. Model. Identif. Control*, 2009, **6**, (3), pp. 196–204

[12] Bansal, R.C., Bhatti, T.S., Kothari, D.R.: 'A novel mathematical modelling of induction generator for reactive power control of isolated hybrid power systems', *Int. J. Model. Simul.*, 2004, **24**, (1), pp. 1–7

[13] Vachirasricirikul, S., Ngamroo, I., Kaitwanidvilai, S.: 'Coordinated SVC and AVR for robust voltage control in a hybrid wind-diesel system', *Energy Convers. Manage.*, 2010, **51**, (12), pp. 2383–2393

[14] GirirajKumar, S.M., Jayaraj, D., Kishan, A.R.: 'PSO based tuning of a PID controller for a high performance drilling machine', *Int. J. Comput. Appl.*, 2010, **1**, (19), pp. 12–17

[15] Demirtas, M.: 'Off-line tuning of a PI speed controller for a permanent magnet brushless DC motor using DSP', *Trans. Energy Convers. Manag.*, 2011, **52**, (1), pp. 264–273

[16] Tlili, I., Timoumi, Y., Nasrallah, S.B.: 'Analysis and design consideration of mean temperature di□erential Stirling engine for solar application', *Renew. Energy*, 2008, **33**, (8), pp. 1911–1921

[17] Kongtragool, B., Wongwises, S.: 'A review of solar-powered Stirling engines and low temperature di□erential Stirling engines', *Renew. Sustain. Energy Rev.*, 2003, **7**, (2), pp. 131–154

[18] Lu, T., Li, N., Zhang, Z., *et al.*: 'Study on the continuous and stable running mode of solar thermal power plant'. Int. Conf. on Sustainable Power Generation and Supply, 2009, pp. 1–4

[19] Mancini, T., Heller, P., Butler, B., *et al.*: 'Dish-Stirling systems: an overview of development and status', *J. Sol. Energy Eng.*, 2003, **125**, (2), pp. 135–151

[20] Abbas, M., Boumeddane, B., Said, N., *et al.*: 'Dish Stirling technology: a 100 MW solar power plant using hydrogen for Algeria', *Int. J. Hydrog. Energy*, 2011, **36**, (7), pp. 4305–4314

[21] Santos-Martin, D., Alonso-Martinez, J., Eloy-Garcia, J., *et al.*: 'Solar dish Stirling system optimisation with a doubly fed induction generator', *IET Renew. Power Gener.*, 2012, **6**, (4), pp. 276–288

[22] Wu, S.Y., Xiao, L., Cao, Y., *et al.*: 'A parabolic dish/AMTEC solar thermal power system and its performance evaluation', *Appl. Energy*, 2010, **87**, (2), pp. 452–462

[23] Jaffe, L.D.: 'Test results on parabolic dish concentrators for solar thermal power systems', *Sol. Energy*, 1989, **42**, (2), pp. 173–187

[24] Reddy, K.S., Veershetty, G.: 'Viability analysis of solar parabolic dish stand-alone power plant for Indian conditions', *Appl. Energy*, 2013, **102**, pp. 908–922

[25] Bansal, R.C.: 'Modelling and automatic reactive power control of isolated wind-diesel hybrid power systems using ANN', *Energy Convers. Manage.*, 2008, **49**, (2), pp. 357–364

[26] Padiyar, K.R.: '*Power systems dynamics, stability and control*' (Interline Publishing, Bangalore, India, 1996)

[27] Bansal, R.C., Bhatti, T.S.: 'Reactive power control of autonomous wind-diesel hybrid power systems using Simulink', *Electr. Power Compon. Syst.*, 2007, **35**, (12), pp. 1345–1366

[28] Elgerd, O.I.: '*Electric energy systems theory an introduction*' (Tata McGraw-Hill Publishing limited, New Delhi, 1983, 2nd edn.)

[29] Bansal, R.C., Bhatti, T.S.: '*Small signal analysis of isolated hybrid power systems: reactive power and frequency control analysis*' (Narosa Publishing House, New Delhi, India, 2008)

[30] Shivakumar, R., Lakshmipathi, R.: 'Implementation of an innovative bio inspired GA and PSO algorithm for controller design considering steam GT dynamics', *Int. J. Comput. Sci.*, 2010, **7**, (1), pp. 18–28

[31] Kamyab, G.R., Fotuhi-Firuzabad, M., Rashidinejad, M.: 'A PSO based approach for multi-stage transmission expansion planning in electricity markets', *Int. J. Electr. Power Energy Syst.*, 2014, **54**, pp. 91–100

[32] Gaing, Z.L.: 'A particle swarm optimization approach for optimum design of PID controller in AVR system', *IEEE Trans. Energy Convers.*, 2004, **19**, (2), pp. 384–391

[33] Das, D.C., Roy, A.K., Sinha, N.: 'GA based frequency controller for solar thermal–diesel–wind hybrid energy generation/energy storage system', *Int. J. Electr. Power Energy Syst.*, 2012, **43**, (1), pp. 262–279

[34] Li, X.Z., Yu, F., Wang, Y.B.: 'PSO algorithm based online self-tuning of PID controller'. IEEE Int. Conf. on Computational Intelligence and Security, 2007, pp. 128–132

[35] Mohanty, S.R., Kishor, N., Ray, P.K.: 'Robust H-infinite loop shaping controller based on hybrid PSO and harmonic search for frequency regulation in hybrid distributed generation system', *Int. J. Electr. Power Energy Syst.*, 2014, **60**, pp. 302–316

[36] Kim, J.S., Kim, J.H., Park, J.M., *et al.*: 'Auto tuning PID controller based on improved genetic algorithm for reverse osmosis plant', *World Acad. Sci. Eng. Technol.*, 2008, **47**, pp. 384–389

[37] Yang, X.S.: 'Flower pollination algorithm for global optimization'. Int. Conf. on Unconventional Computing and Natural Computation, 2012, pp. 240–249

8 Appendix

See Table 7 and 8.

Table 7

Constants	Values
K_1	0.15
K_2	0.793232
K_3	6.22143
K_4	−7.358
K_5	0.126043
K_5'	0.496762
K_5''	−0.122235581
K_6	5.15286
K_7	−3.8347
K_V	0.6667
T_V	0.000106

Table 8

System parameters	
Synchronous generator	
P_{SG}	0.4 p.u. kW
Q_{SG}	0.2 p.u. kVAR
Induction generator	
$P_{IG} = P_{DSTS}$	0.6 p.u. kW
Q_{IG}	0.189 p.u. kVAR
η	80%
P.f	0.9
$x_1 = x_2'$	0.56 p.u.
$r_1 = r_2'$	0.19 p.u.
S	−4.1%
Load	
P_{Load}	1.0 p.u. kW
Q_{Load}	0.75 p.u. kVAR
P.f	0.8
SVC	
Q_{SVC}	0.739 p.u. kVAR
α_o	140.03°
T_α	0.0002 s
T_d	0.001667 s
IEEE type-I excitation system	
K_A	40
T_A	0.05 s
K_F	0.5
T_F	0.715 s
K_E	1.0
S_F	0.0 s